

Oxetane Ring Enlargement through Nucleophilic Trapping of Radical Cations by Acetonitrile

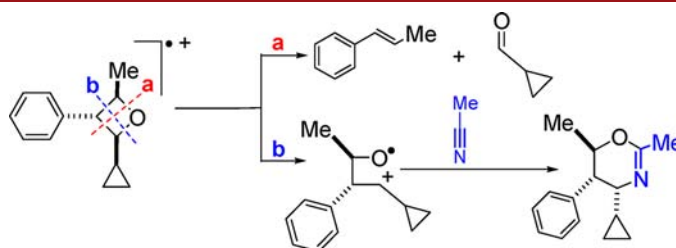
Raúl Pérez-Ruiz,[†] Jose A. Sáez,[†] Luis R. Domingo,[‡] M. Consuelo Jiménez,^{*†} and Miguel A. Miranda^{*†}

Departamento de Química-Instituto de Tecnología Química UPV-CSIC, Universitat Politècnica de València, Camino de Vera s/n, E-46022, Valencia, Spain, and Departamento de Química Orgánica, Universidad de Valencia, Dr. Moliner 50, E-46100 Burjassot, Valencia, Spain

mcjimene@qim.upv.es; mmiranda@qim.upv.es

Received October 2, 2012

ABSTRACT



Oxidative electron transfer cycloreversion of *trans,trans*-2-cyclopropyl-4-methyl-3-phenyloxetane, using triphenylthiapyrylium perchlorate as a photosensitizer, leads to distonic 1,4-radical cations; subsequent cleavage gives rise to fragmentation products (pathway a), whereas nucleophilic trapping by acetonitrile affords a ring expanded oxazine (pathway b).

Photocycloaddition of carbonyl compounds to alkenes (Paterno–Büchi photoreaction) provides a straightforward entry to oxetanes, which are versatile building blocks for organic synthesis.¹ Cycloreversion (CR) of oxetanes can occur through cleavage of the two bonds formed in the photocycloaddition reaction, yielding the starting materials or, more interestingly, the formal metathesis products.² This CR can be initiated by photosensitized electron

transfer (PET), a possibility that has recently attracted considerable interest in connection with its possible involvement in DNA photorepair.^{3–5}

Semiempirical AM1 and PM3 calculations on the photoenzymatic repair of (6-4) DNA photoproducts by photolyases⁶ point to a nonconcerted, two-step mechanism for cleavage of oxetane radical cations *via* initial C–C bond cleavage. In addition, DFT calculations at

[†] Universitat Politècnica de València.

[‡] Universidad de Valencia.

(1) (a) Rix, D.; Ballesteros-Garrido, R.; Zeghida, W.; Besnard, C.; Lacour, J. *Angew. Chem., Int. Ed.* **2011**, *50*, 7308–7311. (b) Burkhard, J. A.; Wuitschik, G.; Rogers-Evans, M.; Mueller, K.; Carreira, E. M. *Angew. Chem., Int. Ed.* **2010**, *49*, 9052–9067. (c) Valiulin, R. A.; Arisco, T. M.; Kutateladze, A. G. *Org. Lett.* **2010**, *12*, 3398–3401. (d) Loy, R. N.; Jacobsen, E. N. *J. Am. Chem. Soc.* **2009**, *131*, 2786–2787. (e) Dussault, P. H.; Trullinger, T. K.; Noor-e-Ain, F. *Org. Lett.* **2002**, *4*, 4591–4593. (f) D'Auria, M. Paternò-Büchi reaction. In *CRC Handbook of Organic Photochemistry and Photobiology*, 3rd ed.; Griesbeck, A., Oelgemöller, M., Ghetti, F., Eds.; CRC Press: Boca Raton, FL, 2012; pp 653–682.

(2) (a) Soicke, A.; Slavov, N.; Neudoerfl, J.-M.; Schmalz, H.-G. *Synlett* **2011**, 2487–2490. (b) D'Auria, M.; Racioppi, R.; Viggiani, L. *Photochem. Photobiol. Sci.* **2010**, *9*, 1134–1138. (c) Valiulin, R. A.; Kutateladze, A. G. *Org. Lett.* **2009**, *11*, 3886–3889. (d) Bach, T. *Liebigs Ann./Recueil* **1997**, 1627–1634. (e) Jones, G., II; Aquadro, M. A.; Carmody, M. A. *J. Chem. Soc., Chem. Commun.* **1975**, 206–207.

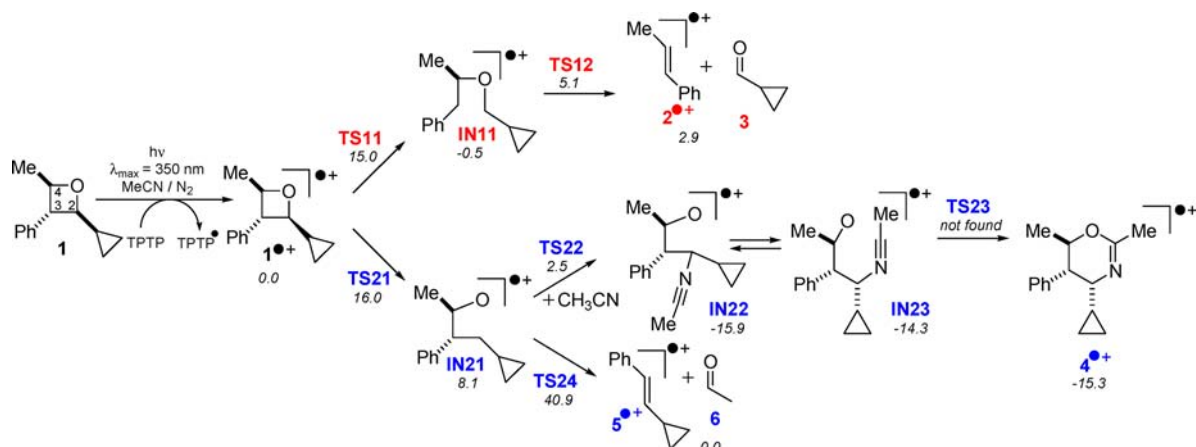
(3) (a) Sadeghian, K.; Bocola, M.; Merz, T.; Schütz, M. *J. Am. Chem. Soc.* **2010**, *132*, 16285–16295. (b) Asgatay, S.; Petermann, C.; Harakat, D.; Guillaume, D.; Taylor, J.-S.; Clivio, P. *J. Am. Chem. Soc.* **2008**, *130*, 12618–12619. (c) Trzcionka, J.; Lhiaubet-Vallet, V.; Paris, C.; Belmadoui, N.; Climent, M. J.; Miranda, M. A. *ChemBioChem* **2007**, *8*, 402–407. (d) Borg, O. A.; Eriksson, L. A.; Durbeej, B. *J. Phys. Chem. A* **2007**, *111*, 2351–2361. (f) Joseph, A.; Falvey, D. E. *Photochem. Photobiol. Sci.* **2002**, *1*, 632. (g) Cichon, M. K.; Arnold, S.; Carell, T. *Angew. Chem., Int. Ed.* **2002**, *41*, 767.

(4) (a) Miranda, M. A.; Izquierdo, M. A.; Galindo, F. *J. Org. Chem.* **2002**, *67*, 4138–4142. (b) Miranda, M. A.; Izquierdo, M. A. *J. Am. Chem. Soc.* **2002**, *124*, 6532–6533. (c) Miranda, M. A.; Izquierdo, M. A. *Photochem. Photobiol. Sci.* **2003**, *2*, 848–850.

(5) (a) Nakabayashi, K.; Kojima, J. I.; Tanabe, K.; Yasuda, M.; Shima, K. *Bull. Chem. Soc. Jpn.* **1989**, *62*, 96–101. (b) Prakash, G.; Falvey, D. E. *J. Am. Chem. Soc.* **1995**, *117*, 11375.

(6) Wang, Y.; Gaspar, P. P.; Taylor, J. S. *J. Am. Chem. Soc.* **2000**, *122*, 5510.

Scheme 1. Analysis of the Reaction Pathways Involving C–C and O–C Bond Breaking of Oxetane Radical Cation $1^{\bullet+}$, in the Absence and in the Presence of Acetonitrile, Together with Selected UMP2/6-31G(d)/PCM(Acetonitrile) Relative Energies (in kcal mol⁻¹)



the UB3LYP/6-31G* level point to CR taking place in a concerted but asynchronous process, where C–C breaking is more advanced than O–C breaking at the transition state.⁷ Experimental work on the PET CR of 2,3-diphenyloxetanes with (thia)pyrylium salts are in better agreement with an initial O–C₂ cleavage.^{4b}

With this background, we have undertaken an experimental and theoretical investigation on the PET CR of oxetane **1**. The choice of **1**, bearing a cyclopropyl group at C₂, was based on several reasons: (i) replacement of H by cyclopropyl in an alkyl cation does not result in a decreased charge density on the involved carbon atom,⁸ (ii) aryl substitution is associated, instead, with the charge delocalization typical of benzylic cations,⁴ and (iii) anodic oxidation of cyclopropylmethyl iodide to the corresponding carbocation, followed by Ritter reaction with acetonitrile and eventual hydrolysis, affords *N*-(cyclopropylmethyl)-acetamide as a trapping product.^{9,10}

The target oxetane **1** was obtained by Paternò–Büchi photocycloaddition of *trans*- β -methylstyrene (**2**) and cyclopropanecarboxaldehyde (**3**). Sensitized photolysis of **1** was performed in the presence of catalytic (10%) amounts of 2,4,6-triphenylthiopyrylium perchlorate (TPTP), in acetonitrile/N₂ at $\lambda_{\text{max}} = 350$ nm (Gaussian distribution). The course of the reaction was followed by GC-MS and ¹H NMR spectroscopy. Conversion of **1** was nearly quantitative after 180 min of irradiation (see Supporting Information, SI, p S18). Three products were found in a photo-mixture: **2** + **3** (35%) and a solvent adduct **4** (60%).

(7) Izquierdo, M. A.; Domingo, L. R.; Miranda, M. A. *J. Phys. Chem. A* **2005**, *109*, 2602–2607.

(8) Tremper, H. S.; Shillady, D. D. *J. Am. Chem. Soc.* **1969**, *91*, 6341–6343.

(9) (a) Laurent, E.; Mison, P.; Thomalla, M. *Comptes Rendus des Seances de l'Academie des Sciences, Serie C: Sciences Chimiques* **1976**, *283*, 601. (b) Laurent, E.; Tardivel, R. *Tetrahedron Lett.* **1976**, *32*, 2779–2782.

(10) (a) Bishop, R. In *Comprehensive Organic Synthesis*; Trost, B. M., Fleming, I., Eds.; Pergamon: Oxford, 1991; Vol. 6, Chapter 1.9. (b) Krimen, L. I.; Coto, N. *J. Org. React. (N. Y.)* **1975**, *17*, 213.

The structure of **4** was assigned as *cis,trans*-4-cyclopropyl-2,6-dimethyl-5-phenyl-4*H*-5,6-dihydro-1,3-oxazine, on the basis of NMR experiments (SI, pp S9–S11) including NOE measurements (SI, pp S12 and S13). These data indicate that H₂, H₃ and the CH₃ group are within the same face of the oxazine plane (Figure 1).

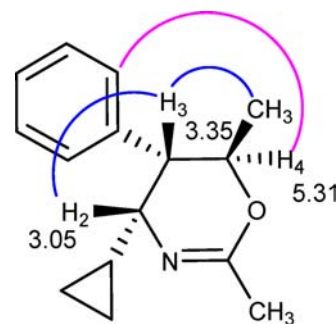


Figure 1. Structural assignment of the acetonitrile adduct **4**. NOE interactions and relevant chemical shifts.

When the PET CR of **1** was performed in deuterated acetonitrile the deuterated analog (*cis,trans*-4-cyclopropyl-2-(methyl-*d*₃)-6-methyl-5-phenyl-4*H*-5,6-dihydro-1,3-oxazine) was obtained (see SI, pp S14–S17). Using benzonitrile as solvent, the corresponding nitrile adduct was also detected by MS ($M^{\bullet+} = 291$, SI, p S19).

To disclose the nature of the TPTP excited state involved in the PET process, quenching experiments were carried out. Thus, the fluorescence intensity of TPTP decreased upon addition of increasing amounts of **1** (Figure 2A). The quenching rate constant $k_q(S_1)$ was obtained from the Stern–Volmer analysis;¹¹ it was found to be $2.6 \times 10^{10} \text{ M}^{-1} \text{ s}^{-1}$,

(11) McNaught, A. D., Wilkinson, A., Eds. *IUPAC Compendium of Chemical Terminology*, 2nd ed.; Royal Society of Chemistry: Cambridge, 1997.

indicating a nearly diffusion-controlled process (Figure 2A, inset). In addition, laser flash photolysis (LFP) of **TPTP** ($\lambda_{\text{exc}} = 355 \text{ nm}$, MeCN/N₂) gave rise to the typical triplet–triplet absorption (Figure 2B, inset); its monitoring at 600 nm, in the presence of **1**, revealed no dynamic quenching, although the end-of-pulse absorbance clearly decreased with increasing concentrations of **1** (Figure 2B). The combined fluorescence and LFP results indicate that the reaction takes place from the singlet excited state of the photosensitizer. This agrees well with the estimation of the free energy changes associated with electron transfer from both excited states (SI, p S21) using the Rehm–Weller relationship.¹²

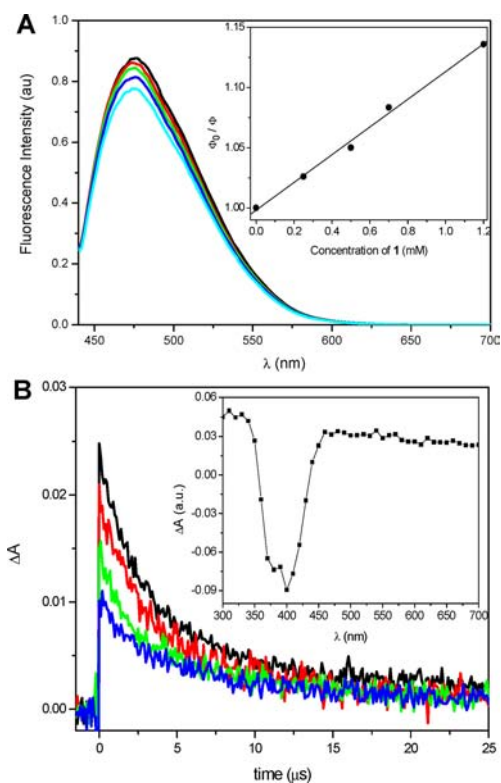


Figure 2. (A) Fluorescence spectra of **TPTP** at 0.03 mM concentration ($\lambda_{\text{exc}} = 435 \text{ nm}$, MeCN/air) in the presence of increasing amounts of **1**; inset: Stern–Volmer plot to obtain $k_q(S_1)$. (B) Decay traces of the T–T absorption of **TPTP** (0.06 mM) measured at 600 nm in the presence of increasing amounts of **1**: 0 mM (black), 1 mM (red), 3.5 mM (green) and 5 mM (blue); inset: transient absorption spectrum of **TPTP** (0.06 mM) recorded 0.2 μs after the laser pulse.

The proposed PET mechanism is outlined in Scheme 1. In principle, cleavage of C₂–C₃ (a) or O–C₂ (b) can occur. Following pathway (a), a distonic 1,4-radical cation with spin and charge located in C₃ and C₂, respectively, would be formed. This should be favored through stabilization of the carbocationic site by oxygen as an oxonium ion. Subsequent O–C₄ bond cleavage would afford **2**^{•+} and **3**;

eventually, back-electron transfer from the thiopyranlyl radical to **2**^{•+} would lead to **2**.¹³ The competitive route (b) would involve formation of a different distonic 1,4-radical cation with spin located in the oxygen and charge in C₂. The higher degree of charge localization in this intermediate would favor nucleophilic attack of acetonitrile at C₂, leading to the corresponding nitrilium derivative; ring closure and back-electron transfer would justify formation of the observed product **4**. The absence of **5** and **6** in the photomixture indicates that trapping of the C₂ located carbocation by acetonitrile occurs faster than C₃–C₄ bond cleavage. In addition, the initial *trans* arrangement of phenyl and cyclopropyl groups in **1** is no longer maintained in **4**, so C₂–C₃ bond rotation must occur along the reaction path.

In order to rule out the possibility that the ring expansion observed under PET conditions results from the well-known acid catalyzed process,¹⁴ due to the presence of adventitious acid traces generated by partial hydrolytic ring opening of **TPTP**, a series of control experiments were performed. Thus, **1** was irradiated in deuterated acetonitrile for 120 min in the presence of **TPTP**, and the reaction mixture was analyzed by ¹H NMR. At this stage, formation of **2**, **3**, and **4**-d₃ was clearly observed (compare Figures 3A and 3B). Interestingly, after an additional 120 min in the dark, no significant changes in the ¹H NMR spectrum were noticed (Figure 3C).

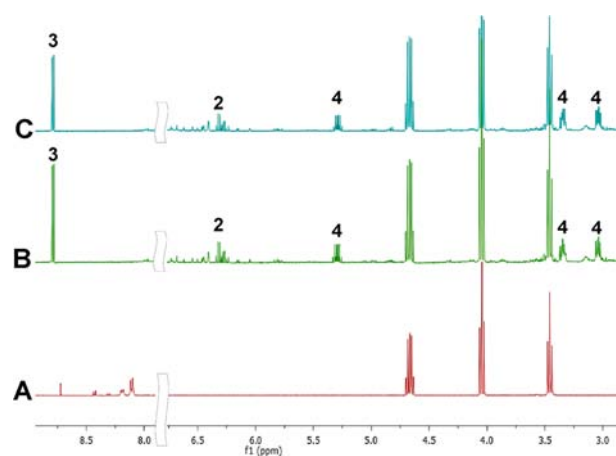


Figure 3. ¹H NMR spectra of deuterated acetonitrile solutions of (A) **1** (8 mM) + **TPTP** (0.8 mM) before irradiation; (B) **1** (8 mM) + **TPTP** (0.8 mM) after 120 min of irradiation at $\lambda_{\text{max}} = 350 \text{ nm}$; and (C) **1** (8 mM) + **TPTP** (0.8 mM) after 120 min of irradiation at $\lambda_{\text{max}} = 350 \text{ nm}$ plus 120 min in the dark.

Conversely, when catalytic amounts of HClO₄ were added to a freshly prepared solution of **1** in the same solvent, ¹H NMR measurements revealed formation of **4**-d₃ and a total absence of **2**, **3**, **5**, or **6**. The results of these control experiments unambiguously prove that different

(13) Izquierdo, M. A.; Miranda, M. A. *Eur. J. Org. Chem.* **2004**, 1424.

(14) Hajnal, A.; Wölling, J.; Schneider, G. *Collect. Czech. Chem. Commun.* **1998**, 63, 1613–1622.

(12) Rehm, D.; Weller, A. *Isr. J. Chem.* **1970**, 8, 259–271.

mechanisms operate in the PET and acid catalyzed processes.

The PET reactions of oxetane **1** were submitted to theoretical calculations at the UMP2(FC)/6-31G(d) level.¹⁵ Due to the intermediacy of positively charged species, solvent effects (acetonitrile) were considered using Tomasi's polarized continuum model (PCM).¹⁶

The stationary points found along the potential energy surface (PES) of the O–C and C–C bond breaking of **1**⁺ are depicted in Scheme 1, together with the corresponding relative energies. Energy profiles of selected reaction paths can be found in Figure 4. Since energy barriers for bond cleavage involving C₄ are between 7 and 15 kcal mol⁻¹ higher than those involving C₂, they will not be discussed further.

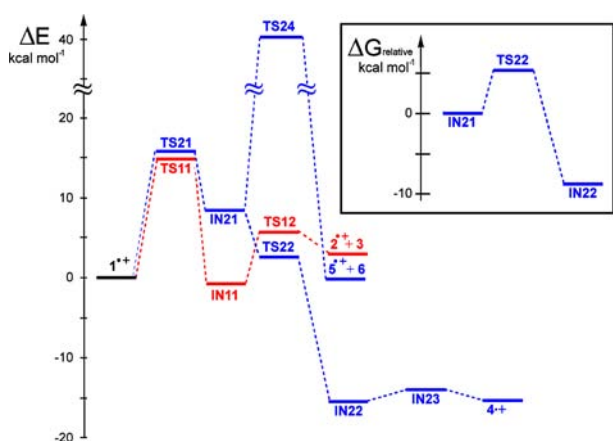


Figure 4. Relative energies of the transition states and intermediates involved in the PET reactions of **1**⁺; inset: relative free energy of transition state, **TS22**.

Starting from **1**⁺, ring splitting to give **2**⁺ + **3** or **5**⁺ + **6**, as well as ring enlargement affording oxazine **4**, takes place via a stepwise mechanism. The initial C₂–C₃ or O–C₂ bond-breaking energy barriers associated with **TS11** and **TS21** are 15.0 and 16.0 kcal mol⁻¹, respectively. Regarding the corresponding intermediates, formation of **IN11** is slightly exothermic (–0.5 kcal mol⁻¹), while that of **IN21** is endothermic (8.0 kcal mol⁻¹). Breaking of the O–C₄ bond at **IN11** yielding **2**⁺ + **3** (which would

complete a formal cycloreversion to the starting materials employed for the Paterno–Büchi synthesis of **1**) proceeds through a barrier of only 5.6 kcal mol⁻¹. The reaction path toward **5**⁺ + **6**, which constitutes a formal metathesis cycloreversion, shares the starting stationary point (**IN21**) with ring enlargement to oxazine **4**⁺. From this saddle point, the energy barrier for C₃–C₄ bond breaking, to give **5**⁺ + **6** through **TS24**, is 32.8 kcal mol⁻¹, which rules out the possibility of formal metathesis cycloreversion. In the presence of acetonitrile as solvent, intermediate **IN21** undergoes a nucleophilic attack at C₂ giving rise to **IN22** via **TS22**. In the energy profile, **TS22** is below **IN21**; however, considering the entropy contribution due the bimolecular nature of this step, a free energy barrier of 5.3 kcal mol⁻¹ is obtained. A conformational equilibrium is established between **IN22** and **IN23** before intramolecular nucleophilic attack, which yields **4**⁺. No transition state **TS23** could be found over the PES at UMP2(FC) level; however, this stationary point was confirmed by using density functional methodology at UB3LYP/6-31G(d)/PCM (acetonitrile) or UM06-2X/6-31G(d)/PCM (acetonitrile) levels. Back-electron transfer (BET) could take place from the thiapyryl radical to **4**⁺ or to **IN23/IN24** to give an alkoxide, which is an excellent nucleophile and would cyclize onto the electron-deficient carbon of the nitrilium moiety in an essentially barrierless process.

To further the energetic discussion, both **TS12** and **TS22** are below the transition states of the first step. Therefore, the kinetic control exerted by the initial ring opening, together with the small energy difference found between **TS11** and **TS21** and the activation barrier of the process yielding **5**⁺ + **6** (formal metathesis), explains the experimentally observed formation of the cycloreversion products **2** and **3**, in addition to oxazine **4**.

In summary, initial O–C₂ bond cleavage of the oxetane ring under PET conditions leads to a distonic 1,4-radical cation, which is trapped by acetonitrile to give a ring expanded oxazine adduct. This is a new reaction, which formally constitutes the creation of a six-membered heterocyclic ring from C=C, C=O, and C≡N units. In addition, splitting of the oxetane radical cation, through stepwise cleavage of the C₂–C₃ and O–C₄ bonds, results in a retro-Paterno–Büchi reaction.

Acknowledgment. Financial support by the MICINN (Grants CTQ-2010-14882, CTQ-2009-13699 and JCI-2010-06204), from CSIC (JAEDOC 101-2011) and from Generalitat Valenciana (Grant No. GV/2012/041-20120205) is gratefully acknowledged.

Supporting Information Available. Additional experimental details, ¹H and ¹³C NMR spectra (including DEPT and NOESY); computational methods; geometry of the stationary points (Cartesian coordinates); structures of the transition states and intermediates involved in the PET CR of **1**. This material is available free of charge via the Internet at <http://pubs.acs.org>.

The authors declare no competing financial interest.

(15) (a) Möller, C.; Plesset, M. S. *Phys. Rev.* **1934**, *46*, 618–622. (b) Head-Gordon, M.; Pople, J. A.; Frisch, M. J. *Chem. Phys. Lett.* **1988**, *153*, 503–506. (c) Saebø, S.; Almlöf, J. *Chem. Phys. Lett.* **1989**, *154*, 83–89. (d) Frisch, M. J.; Head-Gordon, M.; Pople, J. A. *Chem. Phys. Lett.* **1990**, *166*, 275–280. (e) Frisch, M.; Head-Gordon, M.; Pople, J. A. *Chem. Phys. Lett.* **1990**, *166*, 281–289. (f) Head-Gordon, M.; Head-Gordon, T. *Chem. Phys. Lett.* **1994**, *220*, 122–128. (g) *Ab Initio Molecular Orbital Theory*; Hehre, W. J., Radom, L., Schleyer, P. v. P., Pople, A. J., Eds.; Wiley: New York, USA, 1986.

(16) (a) Tomasi, J.; Persico, M. *Chem. Rev.* **1994**, *94*, 2027–2094. (b) *Quantum Chemical and Statistical Theory of Solutions—A Computational Approach*; Simkin, B. Y., Sheikhet, I., Eds.; Ellis Horwood: London, U.K., 1995. (c) Cancès, E.; Mennucci, B.; Tomasi, J. *J. Chem. Phys.* **1997**, *107*, 3032–3041. (d) Cossi, M.; Barone, V.; Cammi, R.; Tomasi, J. *J. Chem. Phys. Lett.* **1996**, *255*, 327–335. (e) Barone, V.; Cossi, M.; Tomasi, J. *J. Comput. Chem.* **1998**, *19*, 404–417.